A Bose-Einstein Condensate of Metastable Atoms

A. Robert, O. Sirjean, A. Browaeys,* J. Poupard,† S. Nowak,‡
D. Boiron, C. I. Westbrook, A. Aspect§

We report the realization of a Bose-Einstein condensate of metastable atoms (helium in the lowest triplet state). The excitation energy of each atom with respect to the ground state is 20 electron volts, but inelastic processes that would destroy the sample are suppressed strongly enough in a spin-polarized sample to allow condensation. Our detection scheme takes advantage of the metastability to achieve detection of individual atoms as well as of the decay products of inelastic processes. This detection opens the way toward new studies in mesoscopic quantum statistical physics, as well as in atomic quantum optics.

Bose-Einstein condensation (BEC) of helium in its ground electronic state has been known for decades and is responsible for many extraordinary properties of liquid helium. The more recently observed BEC of weakly interacting atomic gases exhibits a rich variety of phenomena at the interface between condensed matter and statistical physics on the one hand and atomic, molecular, and quantum optical physics on the other (*1*). The phenomenon has thus far been observed in four different atomic species: H, Li, Na, and Rb (*2*–*5*). We now report the observation of BEC in a fifth species: metastable triplet He (He*). This result is important in itself because not all atoms lend themselves to condensation with present technology and, as was demonstrated in the case of Cs (*6*), sometimes only in attempting to form a BEC can one obtain accurate enough information to conclude whether it is possible or not. In the case of He*, it was in fact predicted that elastic collision rates were sufficiently large and inelastic collision rates were sufficiently low to permit BEC (*7*), and this prediction has stimulated experimental efforts in several labs (*8*–*10*). Our work verifies these predictions, and helium is now the only atom that exhibits BEC in two phases with vastly different densities, corresponding to different electronic states.

A BEC of He* is remarkable in that the constituent atoms contain a large internal energy: the $2\ ^3S_1$ state is 20 eV above the electronic ground state, and this energy is huge compared to the thermal energy of our sample (10^{-10} eV per atom at 1 μK). Only a complete decoupling of the internal and external degrees of freedom prevents conversion of the internal electronic atomic energy into ionization and kinetic energy that would lead to an immediate destruction of the condensate. An unpolarized sample of metastable helium at such a large density (about 10^{13} cm^{-3}) would be destroyed in less than a millisecond (*11*–*13*). The reason this does not happen is the complete spin polarization of a magnetically trapped gas. When all spins are aligned along the same direction, Penning ionizing collisions that could release the internal potential energy are suppressed by spin conservation (*14*). Theoretical studies (*7*, *15*, *16*) that take into account spin relaxation predict a suppression factor as large as 10^5 (*17*).

The large energy content of each atom opens the ultimate possibility of detecting individual atoms with nanosecond time resolution, an extremely challenging task when using optical detection. When the atoms hit a detector such as a microchannel plate (MCP) with a velocity of 1 m/s as in our experiment, the time resolution translates into nanometer position resolution. With such sensitive detection, it will become possible to study mesoscopic statistical physics, with a number of particles ranging from 10^5 or larger to a few, thereby allowing the study of finite number effects in an unusual range (*18*). Individual atom detection will also allow one to perform new quantum atom optics experiments. For instance, the celebrated experiments of spatial interference between two independent condensates (*19*) could be done with a time- and position-resolved detector, so that the emergence of a relative phase between the two condensates, as predicted in several theoretical papers (*20*), could be followed in real time.

Our experiment begins with a magneto-optical trap of He* (*21*). After optical molasses cooling, optical pumping, and magnetic compression, the magnetic trap contains about 2×10^8 atoms at 1 mK. Metastable helium in the $2\ ^3S_1$ state has a (purely electronic) spin of 1, and only the $m = +1$ magnetic sublevel can be trapped. The $m = -1$ sublevel is antitrapped, and $m = 0$ is insensitive to the magnetic field. The magnetic trap is of a "cloverleaf" design (*22*) with $B' = 85$ G/cm, $B'' = 20$ G/cm^2, and a bias field $B_0 = 0.3$ G at the end of the compression. The corresponding axial and radial oscillation frequencies in the harmonic trapping potential are about 50 and 1300 Hz, respectively. The atomic cloud is elongated along the coils' axial direction (Fig. 1), and its lifetime is 50 to 60 s.

After the compression stage, thermalization is rapid enough for evaporative cooling (*21*), and we begin a radio frequency (RF) evaporation ramp at a frequency of 135 MHz. The ramp lasts about 60 s and goes down to a value around 1 MHz, which is about 150 kHz above the minimum of the trapping potential. After the ramp, the trap holds the remaining atoms for 100 ms or more. We then turn off the currents producing the magnetic trap, and atoms falling under the influence of gravity are detected by a MCP placed 5 cm below the trap center. We show in Fig. 2 the signal from the MCP as a function of time after the atoms' release and for various values for the final frequency of the ramp. The time-of-flight (TOF) spectra show the arrival time distribution for a cloud of atoms falling on the detector. The mean arrival time corresponds to the time it takes for the atoms, initially nearly at rest, to fall 5 cm.

Because the width of the distribution is small compared to the mean arrival time, all of the atoms hit the detector with nearly the same final velocity of 1 m/s. The TOF spectra are then proportional to the spatial distribution along the vertical x direction, integrated over y and z.

Figure 2 thus shows the behavior characteristic of most other BEC experiments using atoms in a harmonic trapping potential: At a high final ramp frequency (that is, above the condensation temperature), the spatial distribution is well approximated by a Maxwell-Boltzmann distribution, whereas when the ramp goes low enough and reduces the temperature sufficiently, the distribution exhibits a narrow peak on top of a broad one. The fraction of atoms in the narrow peak increases as the final ramp frequency is lowered, and we interpret this peak as a BEC. The signal disappears altogether when the ramp is allowed to go even lower and to completely empty the trap.

Laboratoire Charles Fabry de l'Institut d'Optique, UMR 8501 du CNRS, Bâtiment 503, Campus Universitaire d'Orsay, Boîte Postale 147, F-91403 Orsay Cedex, France.

*Present address: Laser Cooling and Trapping Group, National Institute of Standards and Technology (NIST), Gaithersburg, MD 20899, USA.
†Present address: R&D Laboratory, GN NETTEST Photonics, Boîte Postale 39, F-78160, Marly le Roi, France.
‡Present address: Bayer Central Research Laboratory, D-51368 Leverkusen, Germany.
§To whom correspondence should be addressed. E-mail: alain.aspect@iota.u-psud.fr

The spectra shown in Fig. 2 correspond to approximately 5×10^3 atoms falling on the MCP. They correspond to freely falling atoms released from the trap immediately after the currents in the coils are turned off. Stray magnetic field gradients are present during the atoms' fall, and therefore we conclude that these atoms are in the field-insensitive $m = 0$ state. We have confirmed this interpretation by deliberately applying a field gradient of 0.1 to 1 G/cm along the vertical direction during the 100-ms fall time. We observed no change in the arrival time nor in the height of the observed peak in the presence of these gradients. We thus interpret the spectra as a sample of the cold, trapped cloud in $m = +1$ (including both the condensed and the uncondensed fractions) that was rapidly transferred to the $m = 0$ state during the switch-off of the current. We know from previous in situ magnetic field measurements that when the current is switched off, eddy currents in the vacuum chamber cause the bias magnetic field at the position of the atoms, originally 0.3 G, to reverse and attain values above 100 G. This reversal takes place in about 100 μs, after which time the magnetic field decays with a time constant of about 1 ms. We presume that during this fast reversal, most of the atomic spins adiabatically follow the magnetic field, but a small fraction ends up in the $m = 0$ state. Such a nonadiabatic transition must take place while the field is close to zero; that is, in a time short compared to the 100-μs reversal time (*23*).

This scenario is supported by two additional observations. First, when applying the vertical gradient mentioned above, we observed a second peak in the TOF spectrum. This peak arrived earlier by an amount consistent with the acceleration caused by the applied gradient and therefore corresponded to atoms in one of the field-sensitive states. This peak had an area as much as seven times greater than that of the $m = 0$ peak, indicating that many more atoms were in the trap than were observed in the TOF spectrum. In a second experiment, we used an RF knife ramping through the trap at 1 kHz/ms to couple the atoms out of the condensate rather than turning off the magnetic field. In this way, we also observed as many as seven times more atoms as in the curves in Fig. 2.

We can confirm the idea that many more atoms are trapped than are observed in Fig. 2 by an independent analysis leading to the number N_{th} of atoms in the thermal cloud below the critical temperature. By fitting the wings of the TOF spectra, we are able to determine the temperature T of the trapped atomic cloud and, using the Bose distribution, to infer N_{th}. As discussed in (*18*) and experimentally demonstrated in (*22*, *24*, *25*), this number should be given by: $N_{th} = 1.202\ (kT/\hbar\tilde{\omega})^3$, where k is Boltzmann's constant, $\hbar$ is Planck's constant divided by 2π, and $\tilde{\omega}$ denotes the geometric mean of the trap oscillation frequencies. This relation gives an absolute thermodynamic measurement of the number of atoms. It is greater by a factor $f = 8 \pm 4$ than the value from the MCP. The uncertainty given for f is the standard deviation of 28 measurements. Taking this correction into account, the largest condensate we have observed contained about 10^5 atoms.

We have also examined the behavior of the condensate for different atom numbers. Figure 3 shows the results of a series of runs for which the number of atoms in the condensate was varied. We plot the width corresponding to the Thomas-Fermi radius of the condensate after expansion, as a function of the number N_0 of atoms in the condensed fraction. We obtained good fits to an inverted parabola squared for numbers of detected atoms as low as 400. The size w_i of the condensate in the direction i, in the Thomas-Fermi approximation, and for a scattering length a is given by

$$w_i = \sigma_i \sqrt{\frac{\tilde{\omega}}{\omega_i}} \left(15 \frac{N_0 a}{\tilde{\sigma}}\right)^{1/5}$$

where $\sigma_i = \sqrt{\{\hbar/m\omega_i\}}$ is the size of the ground state harmonic oscillator wavefunction along the ith direction, and $\tilde{\sigma}$ denotes the geometric mean of the three sizes. To obtain the size of the condensate in the trap from the measured size after the expansion of duration (t) = 100 ms, we use the analysis of (*26*) according to which, for a sudden switch-off of the trapping potential, the spatial distribution of the condensate along an initially tightly confined direction i is simply dilated by a factor $\omega_i t$ during expansion. Thus, the condensate size should vary as the 1/5 power of the number of atoms, as is confirmed by a fit to a log-log plot (slope 0.19) and Fig. 3.

Knowing the size as a function of the number of atoms in the condensate allows

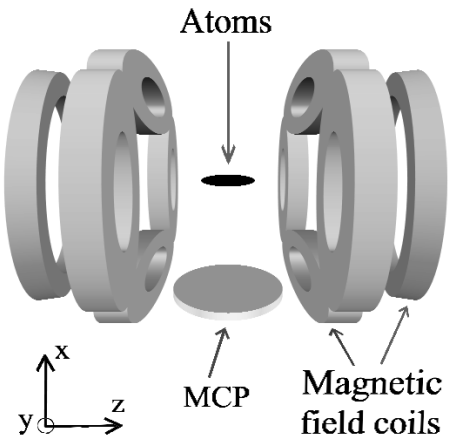

Fig. 1. Schematic diagram of the apparatus (not to scale). The coils that form the magnetic trap are outside the vacuum in reentrant flanges. The microchannel plate is 5 cm below the center of the trap. The incoming He^* beam propagates along the y axis (horizontally). The three pairs of magneto-optical trap laser beams (not shown) propagate along the z axis and at 45° to the x and y axes.

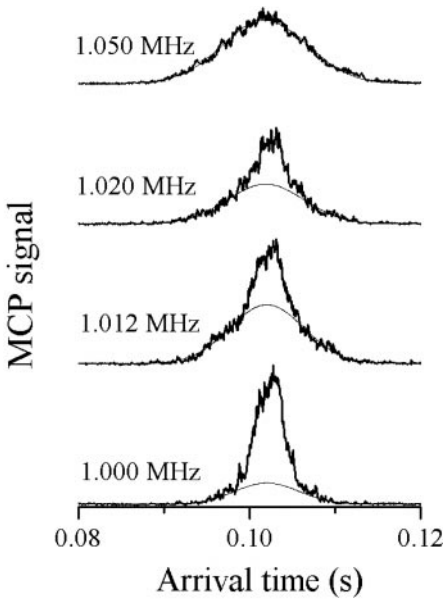

Fig. 2. TOF spectra for different final frequencies of the RF ramp (values are shown at the left of each curve). The solid lines show Gaussian fits to the wings. This series of spectra shows the BEC transition as the RF ramp lowers the temperature further and further. The temperature at the transition is 0.7 μK. Each spectrum is a single-shot acquisition containing about 5×10^3 atoms, although the actual number in the condensate is higher by a factor of about 8.

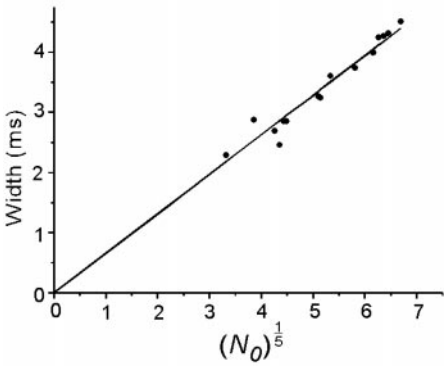

Fig. 3. Observed width of the condensate peak after expansion, as a function of the number of atoms in the peak to the 1/5 power. The width is derived from the TOF spectrum and is given in milliseconds. After correcting the number of atoms for the fraction we do not observe (see text), the slope of the straight line gives an estimate of the scattering length of 20 ± 10 nm.

us also to get an estimate of the scattering length a. We used the data in Fig. 3, and correcting the number of atoms by the correction factor f we obtained $a = 20 \pm 10$ nm. This result is consistent with our elastic rate constant measurements at 1 mK (*21*). The validity of the above analysis relies on two important assumptions. First, the release of the atoms from the trapping potential must be rapid as compared to the inverse of the angular frequency ω_i. If this were not the case, the expansion would not be as fast as expected, and this discrepancy would lead to an underestimate of the size of the condensate and therefore of a. According to the discussion of the rapid transfer to $m = 0$ above, it is reasonable to believe that the condition is fulfilled in our case, but its violation can lead to large errors. The second assumption is that the interaction energy between the atoms in the various m sublevels is described by a single scattering length a (*27*, *28*) and that they all expand freely (*29*).

We have also observed the ions produced by the trapped condensate by negatively biasing a grid above the MCP (Fig. 4). These ions are due to Penning ionization of residual gases, two-body Penning collisions within the condensate, or possibly to other, more complicated processes. We observed a factor of 4 to 5 more ions from the condensate than from a thermal cloud at 1 μK, and we attribute this increase to the larger density in the condensate. The lifetime of the condensate, estimated by observing the decay of the ion rate, is on the order of a few seconds. This is true both with and without an RF knife to evacuate hot atoms (*22*, *30*), although the lifetime is slightly longer with the knife present. The density of the condensate, deduced from its vertical size measurement and its known aspect ratio, is on the order of 10^{13} cm^{-3}, so from the lifetime we can place an upper limit of 10^{-13} cm^3 s^{-1} on the relaxation-induced Penning ionization rate constant.

The observation of BEC in He*, together with our MCP detector, offers many new possibilities for the investigation of BECs. The ion detection described in the previous paragraph allows continuous nondestructive monitoring of the trapped condensate. Our ability to count individual He* atoms falling out of the trap can be combined with several outcoupling schemes releasing the atoms in the field-insensitive $m = 0$ state: A laser-induced Raman transition (*31*) can provide an even faster and more flexible scheme than the fast reversal of the magnetic field presented here; on the other hand, like an RF outcoupler, it can also produce a quasi–continuous-wave atom laser (*32*, *33*), and the RF experiment presented above is a crude version of it. Fast dumping of atoms, with numbers ranging from over 10^5 to a few, can offer new opportunities for studies in statistical physics with low numbers of particles, such as investigations of corrections far from the thermodynamical limit (*18*). Slow outcoupling combined with space- and time-resolved detection of individual atoms should allow one to perform accurate comparisons of correlation functions (*30*) for a thermal beam of ultracold atoms (*34*) and for an atom laser, realizing the quantum atom optics counterpart of one of the fundamental experiments of quantum optics. Experiments that are still unrealized in quantum photon optics may also become possible with a system such as that reported here.

It has already been shown that the laser and vacuum apparatus necessary to manipulate ^{4}He is readily adapted to the fermionic isotope ^{3}He (*12*). Thus we expect that it will soon be possible to study a degenerate gas of fermions using sympathetic cooling (*35*–*37*). Finally, the upper-lying levels of triplet metastable helium are radiatively coupled to the electronic $1\,^1S_0$ ground state, so that a laser excitation of the condensate toward one of these levels would create a population inversion with the ground state. This excitation could lead to superradiance, and even lasing beyond 20 eV. It might also yield a dilute degenerate sample of ground-state helium, giving yet a third phase of quantum degenerate helium.

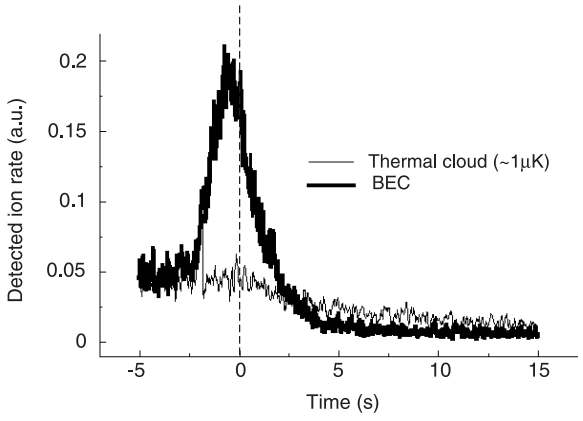

Fig. 4. Ions detected by the MCP during the magnetic trap phase. The vertical dashed line at $t = 0$ corresponds to the end of the RF ramp. The thin line corresponds to a final RF frequency of 1.2 MHz (Fig. 2) [that is, a thermal cloud ($T = 1$ μK)], whereas for 0.97 MHz (thick line) the cloud is almost a pure BEC. The lifetime is smaller in the latter case, indicating a higher loss rate for a BEC.

References and Notes

1. *Proceedings of the International School of Physics "Enrico Fermi," Course CXL*, M. Inguscio, S. Stringari, C. E. Wieman, Eds. (IOS Press, Amsterdam, 1999).
2. M. H. Anderson, J. R. Ensher, M. R. Matthews, C. E. Wieman, E. A. Cornell, *Science* **269**, 198 (1995).
3. K. B. Davis *et al.*, *Phys. Rev. Lett.* **75**, 3969 (1995).
4. C. C. Bradley, C. A. Sackett, J. J. Tollet, R. G. Hulet, *Phys. Rev. Lett.* **75**, 1687 (1995).
5. D. G. Fried *et al.*, *Phys. Rev. Lett.* **81**, 3811 (1998).
6. D. Guéry-Odelin, J. Söding, P. Desbiolles, J. Dalibard, *Europhys. Lett.* **44**, 25 (1998).
7. G. V. Shlyapnikov, T. M. Walraven, U. M. Rahmanov, M. W. Reynolds, *Phys. Rev. Lett* **73**, 3247 (1994).
8. W. Vassen, *OSA TOPS on Ultracold Atoms and BEC* **7**, 20, K. Burnett, Ed. (Optical Society of America, Washington, DC, 1996).
9. F. Pereira Dos Santos *et al.*, *Euro. Phys. J. D.* **14**, 15 (2001).
10. H. C. W. Beijerinck, E. J. D. Vredenbregt, R. J. W. Stas, M. R. Doery, J. G. C. Tempelaars, *Phys. Rev. A* **61**, 023607 (2000).
11. H. C. Mastwijk, J. W. Thomsen, P. van der Straten, A. Niehaus, *Phys. Rev. Lett.* **80**, 5516 (1999).
12. M. Kumakura, N. Morita, *Phys. Rev. Lett.* **82**, 2848 (1999).
13. P. J. J. Tol, N. Herschbach, E. A. Hessels, W. Hogervorst, W. Vassen, *Phys. Rev. A* **60**, R761 (1999).
14. For two colliding spin-polarized atoms, the initial value of the total spin is 2, whereas the final value cannot be larger than 1 for the products of Penning ionization, a ground-state helium atom with zero spin, a He^+ ion with spin 1/2, and an electron with spin 1/2.
15. P. O. Fedichev, M. W. Reynolds, U. M. Rahmanov, G. V. Shlyapnikov, *Phys. Rev. A* **53**, 1447 (1996).
16. V. Venturi, I. B. Whittingham, P. J. Leo, G. Peach, *Phys. Rev. A* **60**, 4635 (1999).
17. This suppression is particularly remarkable in He*. For instance, it has not been observed in Xe* [C. Orzel, M. Walhout, U. Sterr, P. S. Julienne, S. L. Rolston, *Phys. Rev. A* **59**, 1926 (1999)].
18. F. Dafolvo, S. Giorgini, L. P. Pitaevskii, S. Stringari, *Rev. Mod. Phys.* **71**, 463 (1999) and references therein.
19. M. R. Andrews *et al.*, *Science* **275**, 637 (1997).
20. See, for example, P. Horak, S. M. Barnett, *J. Phys. B* **32**, 3421 (1999) and references therein.
21. A. Browaeys *et al.*, in preparation.
22. M.-O. Mewes *et al.*, *Phys. Rev. Lett.* **77**, 416 (1996).
23. If the field passes almost exactly through zero during reversal, most of the atoms would become anti-aligned with the field, but also in this case a small fraction would end up in the $m = 0$ state, and this transfer would again take place in significantly less than the total reversal time.
24. L. V. Hau *et al.*, *Phys. Rev. A* **58**, R54 (1998).
25. J. R. Ensher, D. S. Jin, M. R. Matthews, C. E. Wieman, E. A. Cornell, *Phys. Rev. Lett.* **77**, 4984 (1996).
26. Y. Castin, R. Dum *Phys. Rev. Lett.* **77**, 5315 (1996).
27. Theoretical arguments support this assumption [P. Leo, E. Tiesinga, personal communication].
28. P. J. Leo, V. Venturi, I. B. Whittingham, J. F. Babb, in preparation.
29. This is a reasonable assumption because, in a cloverleaf trap, an increase of the bias field results in a dramatic decrease of the stiffness of the potential, so that a few microseconds after the partial transfer to $m = 0$, atoms in $m = \pm 1$ can also be considered free at the scale of the interaction energy. Otherwise, one would have to take into account a correction factor not larger than 2 [see reference 20 in (*31*)].
30. E. A. Burt *et al.*, *Phys. Rev. Lett.* **79**, 337 (1997).
31. E. Hagley *et al.*, *Science* **283**, 1706 (1999).
32. I. Bloch, T. W. Hänsch, T. Esslinger, *Nature* **403**, 166 (2000).
33. F. Gerbier, P. Bouyer, A. Aspect, *Phys. Rev. Lett.*, in press (and references therein).
34. Y. Yasuda, F. Shimizu, *Phys. Rev. Lett.* **77**, 3090 (1996).

35. B. DeMarco, D. S. Jin, *Science* **285**, 1703 (1999).
36. F. Schreck *et al.*, in preparation.
37. A. G. Truscott, K. E. Strecker, W. I. McAlexander, G. B. Partridge, R. G. Hulet, *Science* 1 March 2001 (10.1126/science.1059318).
38. During the preparation of this manuscript, we learned that the He* group at the Ecole Normale Supérieure, Paris, also observed BEC [F. Pereira Dos Santos *et al.*, *Phys. Rev. Lett* **86**, 3459 (2001)]. We thank the NIST Laser Cooling and Trapping and Quantum Processes groups and G. Shlyapnikov for helpful discussions and A. Villing and F. Moron for invaluable assistance. Supported by the European Union under grants IST-1999-11055 and HPRN-CT-2000-00125, and by the Direction Générale de l'Armement grant 99.34.050.

12 March 2001; accepted 16 March 2001
Published online 22 March 2001;
10.1126/science.1060622
Include this information when citing this paper.

HIFα Targeted for VHL-Mediated Destruction by Proline Hydroxylation: Implications for O_2 Sensing

Mircea Ivan,[1] Keiichi Kondo,[1] Haifeng Yang,[1] William Kim,[1] Jennifer Valiando,[1] Michael Ohh,[1] Adrian Salic,[3] John M. Asara,[4] William S. Lane,[4] William G. Kaelin Jr.[1,2]*

HIF (hypoxia-inducible factor) is a transcription factor that plays a pivotal role in cellular adaptation to changes in oxygen availability. In the presence of oxygen, HIF is targeted for destruction by an E3 ubiquitin ligase containing the von Hippel–Lindau tumor suppressor protein (pVHL). We found that human pVHL binds to a short HIF-derived peptide when a conserved proline residue at the core of this peptide is hydroxylated. Because proline hydroxylation requires molecular oxygen and Fe^{2+}, this protein modification may play a key role in mammalian oxygen sensing.

How cells sense changes in ambient oxygen is a central question in biology. In mammalian cells, lack of oxygen, or hypoxia, leads to the stabilization of a sequence-specific DNA binding transcription factor called HIF, which transcriptionally activates a variety of genes linked to processes such as angiogenesis and glucose metabolism (*1–4*). HIF binds to DNA as a heterodimer consisting of an α subunit and a β subunit.

Von Hippel–Lindau (VHL) disease is a hereditary cancer syndrome characterized by the development of highly vascular tumors that overproduce hypoxia-inducible mRNAs such as vascular endothelial growth factor (VEGF) (*5*). The product of the VHL tumor suppressor gene, pVHL, is a component of a multiprotein complex that bears structural and functional similarity to SCF (Skp1/Cdc53 or Cullin/F-box) ubiquitin ligases (*6–11*). In the presence of oxygen, pVHL, in association with elongin B and elongin C, binds directly to HIFα subunits and targets them for polyubiquitination and destruction (*7–10*). Cells lacking functional pVHL cannot degrade HIF and thus overproduce mRNAs encoded by HIF target genes (*12*). Here, we investigate the mechanism by which hypoxia prevents the destruction of HIF.

VHL interacts with a modified form of HIF. We first followed up on earlier observations that cobalt chloride or iron chelators such as desferrioxamine (i) stabilize HIF and lead to transcriptional activation of its target genes (*1–4*), (ii) inhibit the binding of pVHL to HIF (*12*), and (iii) inhibit HIF polyubiquitination by pVHL in vitro (*7*). To study this further, we treated pVHL-defective renal carcinoma cells with increasing amounts of cobalt chloride or desferrioxamine. As shown earlier, the untreated cells contained high levels of HIF-2α, which bound directly to recombinant pVHL–elongin B–elongin C (VBC) (*7, 12, 13*) (Fig. 1A). In contrast, VBC did not recognize HIF-2α isolated from cells treated with cobalt chloride or desferrioxamine.

A recent study indicated that hypoxia, in contrast to cobalt chloride and desferrioxamine, inhibits HIF polyubiquitination but not the physical association of pVHL and HIF (*12*). This suggests that physiological regulation of HIF by hypoxia is mechanistically distinct from the pharmacological effects of cobalt chloride and desferrioxamine. Exposure of cell extracts to oxygen in this earlier study, however, might have allowed for reformation of pVHL-HIF complexes after lysis. To explore these observations further, we grew mouse cells (ts20) with a temperature-sensitive mutation in the E1 ubiquitin-activating enzyme (*14*) at the nonpermissive temperature under hypoxic or normoxic conditions so that HIF would accumulate in the presence or absence of oxygen (*15*). Although comparable levels of HIF accumulated in these two settings, VBC only recognized the HIF from normoxic cells (Fig. 1B). Thus, the interaction of pVHL with HIF appears to be governed by a posttranslational modification of HIF that is oxygen- and iron-dependent.

pVHL binds to a region of HIF-1α called the oxygen-dependent degradation domain (ODD) (*7*). We had observed that pVHL bound to HIF produced in rabbit reticulocyte lysate but did not bind to HIF produced in wheat germ extracts or in *Escherichia coli* (*16*). Furthermore, wheat germ– or *E. coli*–derived HIF acquired pVHL binding activity after preincubation with human, rabbit, or *Xenopus* cell extracts at 37°C (*16*). For example, glutathione *S*-transferase (GST)–ODD fusion proteins produced in *E. coli* were not recognized by VBC unless preincubated with a rabbit reticulocyte lysate (Fig. 1C). VBC did not recognize GST-ODD fusion proteins incubated with a heat-inactivated reticulocyte lysate (Fig. 1D). These results indicate that pVHL recognizes a modified form of HIF and that this modification is carried out by a factor present in a variety of vertebrate cell extracts.

To determine the nature of this modification, we first narrowed the region of HIF that binds to pVHL. Gal4-HIF fusion proteins containing HIF residues 555 to 575 bound specifically to immobilized GST-VBC complexes (Fig. 2, A and E) (*13, 17*). Likewise, a biotinylated peptide corresponding to HIF residues 556 to 575 [henceforth HIF(556-575)] bound to pVHL after preincubation with reticulocyte lysate (Fig. 2B) (*18*). As noted by others, this region of HIF contains a highly conserved collinear sequence, Met-Leu-Ala-Pro-Tyr-Ile-Pro-Met (Fig. 2E), which, when mutated to eight consecutive alanines, leads to HIF stabilization (*19*). An alanine scan of this region showed that Leu^{562} and Pro^{564} were essential for specific binding to pVHL (Fig. 2B). In contrast, mutation of the one potential phosphoacceptor in this peptide, Tyr^{565}, did not affect pVHL binding, consistent with an earlier study in which a $Tyr^{565} \rightarrow$ Phe mutation did not affect HIF stability (*20*). Moreover, phosphatase treatment did not affect the binding of pVHL to GST-ODD in these assays (*16*).

Mutation of either Leu^{562} or Pro^{564} to Ala in the context of full-length HIF-1α or a Gal4-ODD fusion protein abrogated pVHL

[1]Dana-Farber Cancer Institute and Brigham and Women's Hospital, [2]Howard Hughes Medical Institute, Harvard Medical School, 44 Binney Street, Boston, MA 02115, USA. [3]Department of Cell Biology, Harvard Medical School, Boston, MA 02115, USA. [4]Microchemistry and Proteomics Analysis Facility, Harvard University, Cambridge, MA 02138, USA.

*To whom correspondence should be addressed. E-mail: william_kaelin@dfci.harvard.edu

A Bose-Einstein Condensate of Metastable Atoms

A. Robert, O. Sirjean, A. Browaeys, J. Poupard, S. Nowak, D. Boiron, C. I. Westbrook, and A. Aspect

Science, 292 (5516), • DOI: 10.1126/science.1060622